III International Conference on Particle-based Methods – Fundamentals and Applications
PARTICLES 2013
M. Bischoff, E. Oñate, D.R.J. Owen, E. Ramm & P. Wriggers (Eds)

COUPLING OF THE MESHLESS SPH-ALE METHOD WITH A FINITE VOLUME METHOD

MAGDALENA NEUHAUSER[1], JEAN-CHRISTOPHE MARONGIU[2] AND FRANCIS LEBOEUF[1]

[1] Laboratory of Fluid Mechanics and Acoustics
Ecole Centrale de Lyon
36 Avenue Guy de Collongue, Ecully, France
Magdalena.Neuhauser@ec-lyon.fr

[2] Competence Center ASPHODEL
ANDRITZ Hydro SAS
13 Avenue Albert Einstein, Villeurbanne, France
Jean-Christophe.Marongiu@andritz.com

Key words: SPH-ALE, Finite Volume, coupling, CFD

Abstract. This paper presents a novel coupling algorithm for a Smoothed Particle Hydrodynamics-Arbitrary Lagrange Euler (SPH-ALE) and a mesh-based Finite Volume (FV) method where information is transferred in two ways. On the one hand, we use the FV calculation points as SPH neighbors in the regions where the mesh is overlapping the SPH-ALE particles. On the other hand, the boundary conditions for the FV domain are interpolated from the SPH-ALE particles, similar to what is done in the CHIMERA method of overlapping meshes. In contrast to the CHIMERA method, interpolation is not performed on a structured grid but on a set of unstructured points. Hence, an interpolation technique for scattered data is used. The approach is carefully validated by means of well-known academic testcases that show very encouraging results. Our final aim is the simulation of transient flows in hydraulic machines.

1 INTRODUCTION

The meshless method Smoothed Particle Hydrodynamics - Arbitrary Langrange Euler (SPH-ALE) is very well adapted for the simulation of highly dynamic free surface flows with moving geometries. In the past years, increasing computational power opened the door to real industrial applications like for example the flow in the casing of a Pelton turbine shown in Figure 1, computed within the Research & Development Department of ANDRITZ Hydro. However, the approach has rarely been applied to internal flows because it has difficulties to correctly represent rapidly changing gradients of the field variables like they typically occur close to wall boundaries [1]. In mesh-based methods a

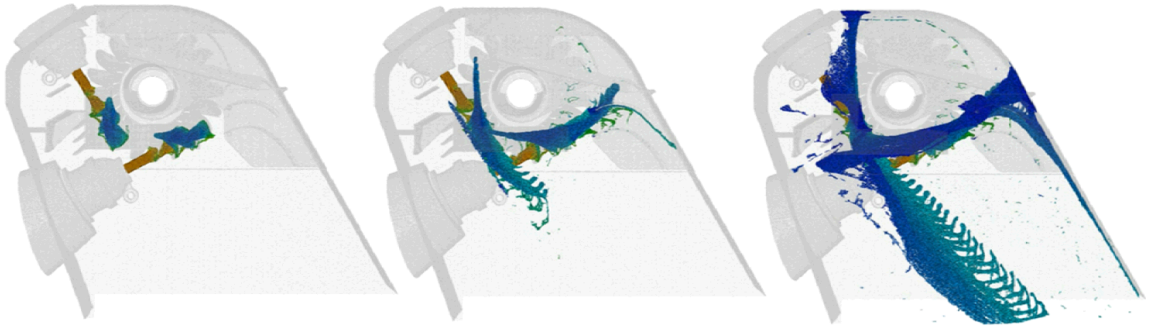

Figure 1: Free surface flow in the casing of a Pelton turbine computed with SPH-ALE at three different instants. High velocity is colored in red and low velocity in blue [2].

non-constant spatial discretization size is used and the mesh is strongly refined in these regions. The equivalence for SPH, particle refinement, is difficult to implement if particles are moving in Lagrangian motion and the isotropic nature of most SPH formalisms makes it complicated to refine particles in an anisotropic way, like it is for example done for solving boundary layers with mesh-based methods.

Finite Volume (FV) methods are well established in CFD because of their accuracy and stability. However, they can be tedious for simulations with moving geometries and free surfaces. In addition, they often necessitate an interface between moving and static parts of the mesh which introduces additional errors. To overcome the shortcomings of both methods, we propose a coupling where we use SPH-ALE in the whole computational domain and an overlapping FV mesh in regions where a refined solution is desired.

2 NUMERICAL METHODS

Considering the weakly-compressible Euler equations in an arbitrarily moving frame of reference, an SPH and a FV method are derived that are then used for the coupling.

2.1 SPH-ALE

SPH was first introduced in 1977 by Lucy [3] and Gingold and Monaghan [4] for astrophysical applications and was then further developed for fluid applications. The computational domain is discretized by a set of unstructured points without any connectivity, called particles. The value of a function $f(x)$ at a point i is computed by convolution with a kernel function W and we obtain the following discrete form,

$$\langle f(x_i) \rangle = \sum_{j \in D_i} \omega_j f(x_j) W_{ij}. \tag{1}$$

The kernel support area of particle i is denoted by D_i and $W_{ij} = W(x_j - x_i, h)$ is the kernel function evaluated at the distance between two particles i and j and depending on

the smoothing length h that determines the size of the kernel support. The integration weight ω_j is the volume of particle j. Applying partial integration, we obtain the following formula for the gradient of a function f that is valid far away from wall boundaries,

$$\langle \nabla f(x_i) \rangle = \sum_{j \in D_i} \omega_j f(x_j) \nabla W_{ij}, \tag{2}$$

where the gradient of the kernel function can be computed analytically. Eq. (2) is used to discretize the fluid equations, where a strong point of this method is that the particles move with the flow in Lagrangian motion. The approach is therefore able to capture free surfaces easily. In 1999 Vila [5] introduced SPH-Arbitrary Lagrange Euler (ALE) which is a more accurate and stable variant of SPH. The starting point is a conservative formulation of the Euler equations, written in an arbitrarily moving frame of reference,

$$L_{v_0}(\Phi) + \nabla \cdot F(\Phi, v_0) = Q, \tag{3}$$

with

$$F(\Phi, v_0) = F_E(\Phi) - v_0 \Phi, \tag{4}$$

where Φ denotes the vector of the conservative variables, $F_E(\Phi)$ the vector of the Euler fluxes, Q the source term and L_{v_0} is the transport operator associated with the transport field v_0. A system of SPH equations is obtained that is quite similar to finite volume formulations. Riemann solvers are introduced and mass can be exchanged between pairs of particles. That means that particles should be rather considered as moving control volumes than particles, even if we continue to call them particles to underline the meshless character of the method. We obtain the following discrete SPH-ALE formulation of the weakly compressible Euler equations,

$$\begin{cases} \dfrac{d}{dt}(x_i) = v_0(x_i, t), \\ \dfrac{d}{dt}(\omega_i) = \omega_i \displaystyle\sum_{j \in D_i} \omega_j (v_0(x_j) - v_0(x_i)) \nabla W_{ij}, \\ \dfrac{d}{dt}(\omega_i \rho_i) = -\omega_i \displaystyle\sum_{j \in D_i} \omega_j 2 \rho_{ij}^E \left(v_{ij}^E - v_0(x_{ij}, t) \right) \cdot \nabla W_{ij}, \\ \dfrac{d}{dt}(\omega_i \rho_i v_i) = -\omega_i \displaystyle\sum_{j \in D_i} \omega_j 2 \left[\rho_{ij}^E v_{ij}^E \otimes (v_{ij}^E - v_0(x_{ij}, t)) + p_{ij}^E \right] \cdot \nabla W_{ij} + \omega_i \rho_i g, \end{cases} \tag{5}$$

where $\rho(x,t)$ is the density, $p(x,t)$ the pressure, $v(x,t)$ the flow velocity and g the gravity. The system of equations is closed by a weakly compressible state equation, often referred to as Tait's equation,

$$p_i = \frac{\rho_0 c_0}{\gamma} \left[\left(\frac{\rho_i}{\rho_0} \right)^\gamma - 1 \right], \tag{6}$$

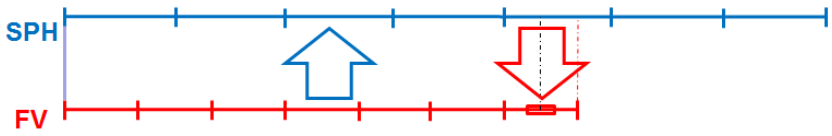

Figure 2: Sketch of the coupling algorithm. FV calculation points are used as SPH neighbours, while FV boundary values are interpolated from SPH particles.

where $\gamma = 7$ and ρ_0 and c_0 denote the reference density and the reference speed of sound, respectively. The v_{ij}^E, ρ_{ij}^E and p_{ij}^E are the solutions of a moving Riemann problem between two particles obtained with approximate linearized Riemann solvers that are computationally less expensive than iterative solvers. The transport field v_0 is the particle velocity and can be chosen freely. If the particle velocity is chosen equal to the fluid velocity $v_0 = v$ we obtain a Lagrangian description as in standard SPH, if we set $v_0 = 0$ we obtain an Eulerian description as in many classical mesh-based methods. However, we can also choose an arbitrary particle velocity, for example following the movement of the solid geometries (cf. [1]). For more information about SPH-ALE see [6, 7].

2.2 Finite Volume solver

Starting from the same set of Euler equations in an arbitrary frame of reference Eq. (3) as in the above section, the semi-discrete flow equations in conservation form for FV schemes can be written as

$$\frac{d}{dt}(\Phi_l V_l) + \sum_{sides}(\hat{F}(\Phi, v_0) \cdot S) = Q_l V_l, \tag{7}$$

where we sum over the flux terms of the sides of cell l. The $\Phi_l = (\rho_l, \rho_l v_l)^T$ denotes the state vector of cell l, V_l its volume and $\hat{F}$ the numerical flux of Eq. (4) through the sides with surface S and Q_l the source term. For more information about FV methods see for example [8]. In this paper we use a one-dimensional weakly compressible inviscid in-house FV solver that is very similar to the above described SPH-ALE formalism. The same linearized Riemann solver, the same time integration scheme, the same reconstruction of the state variable for the Riemann solver and the same state equation are used.

3 THE COUPLING ALGORITHM

In the following, we assume that the whole computational domain is covered by SPH particles that are overlapped by FV meshes in regions where a refinement is necessary. The flow information has to be transferred in two ways, indicated by two arrows in Figure 2. On the one hand the FV calculation points are used as SPH neighbors in the overlapping regions, while on the other hand the boundary values for the FV domain are interpolated from the SPH particles.

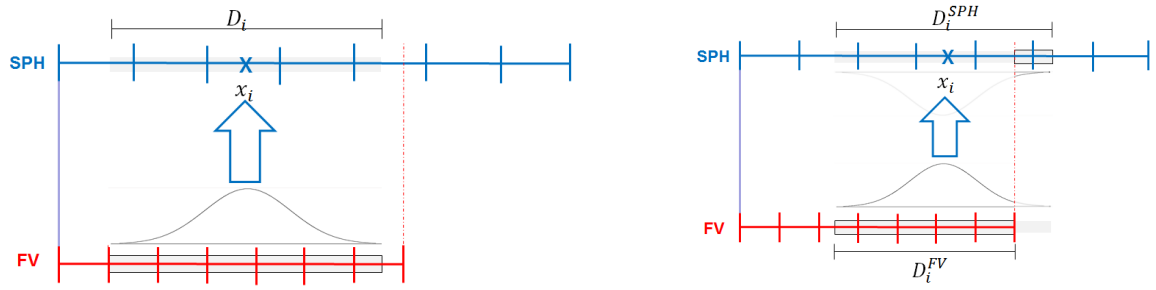

(a) Only FV calculation points are acting as SPH neighbours.

(b) FV and SPH calculation points are acting as SPH neighbours.

Figure 3: Sketch of the coupling algorithm: Integration in the SPH domain.

3.1 Information transfer from FV to SPH-ALE

In the above section we explain that the FV meshes are added to the SPH simulation for local refinement. Thus, we can assume that the physical fields, computed by the FV solver, are the more accurate ones. Therefore, the FV calculation points are used as neighbors for the SPH integration in the overlapping region. Figure 3(a) illustrates the transfer and shows that the smoothing length is determined by the SPH discretization size. In Figure 3(b) the considered SPH particle is situated close to the boundary of the FV domain. Its kernel support traverses the FV domain, so that FV calculation points as well as SPH particles have to be considered as neighbors. If the boundary of the FV mesh does not coincide with the interfaces between particles, SPH particles have to be cut in order to obtain a correct space discretization for the integration over the neighbors, as indicated in Figure 4. Consider the example of Figure 4. The modified volume of the cut particle $\bar{\omega}_i$ is equal to the difference between the volume of the original particle and the volume of the finite volume cells that are overlapping the original particle. Hence, we obtain $\bar{\omega}_i = \omega_i - (V_{l_1} + V_{l_2})$. In the general case, we write

$$\bar{\omega}_i \approx \begin{cases} \omega_i - \sum_l V_l, & (\omega_i - \sum_l V_l) > 0 \\ 0, & \text{elsewhere.} \end{cases} \tag{8}$$

It is known that in SPH the errors increase significantly if particles are not situated at their barycenters [9]. For that reason a correction of the position of the cut particles is applied. We reconsider the example in Figure 4. If we assume that the particles are situated at their barycenters in the beginning, we know from the definition of the barycenter that the modified position $\bar{x}_i$ can be expressed as $\bar{x}_i = \frac{1}{\bar{\omega}_i}(x_i\omega_i - (x_{l_1}V_{l_1} + x_{l_2}V_{l_2}))$. In the general case, we have

$$\bar{x}_i \approx \frac{1}{\bar{\omega}_i}\left(x_i\omega_i - \sum_l x_l V_l\right) \tag{9}$$

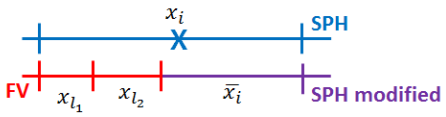

Figure 4: Example of an SPH particle (indicated in blue) that is partially overlapped by FV cells (in red). The modified SPH particle for the integration over neighbouring particles is indicated in purple.

In summary, we obtain the coupled SPH flow equations that are written as

$$\frac{d(\omega_i \Phi_i)}{dt} = \omega_i \left(\sum_{l \in D_i^{FV}} V_l F_{il} \nabla W_{il} + \sum_{j \in D_i^{SPH}} \bar{\omega}_j F_{ij} \nabla W_{ij} \right), \tag{10}$$

where $\bar{\omega}_j$ denotes the modified weights, Φ_i the vector of state variables of particle i and F_{ij} the numerical flux between calculation points i and j. Note that $\bar{\omega}_j = 0$ if particle j is completely overlapped by FV cells and $\bar{\omega}_j = \omega_j$ if the particle is not at all overlapped. That ensures a correct space discretization of the computational domain for the SPH integration over the neighbors. The kernel support area of particle i in the FV domain is denoted by D_i^{FV} and in the SPH domain by D_i^{SPH}. As mentioned above, in both cases the smoothing length h is determined by the SPH particle size.

3.2 Information transfer from SPH-ALE to FV

The FV mesh that is overlapping the SPH particles is used for refinement, to obtain a more accurate solution. Boundary values have to be imposed to this domain. Therefore, velocity and density are interpolated from the SPH points similar to the CHIMERA method of overlapping grids [10, 11]. In contrast to the CHIMERA method where the interpolation is performed on blocks of structured grids, the fields are interpolated from a set of unstructured SPH particles and scattered data approximation techniques have to be used like Shepard interpolation or higher order moving least square (MLS) interpolation.

4 TESTCASES

4.1 Sinusoidal initial velocity

Figure 5 shows the velocity of a one-dimensional coupled simulation where a sinusoidal velocity is imposed at the inlet of the domain, situated at $x = 0$, and constant static pressure at the outlet. We use 50 SPH particles distributed in the whole computational domain and 50 FV cells distributed in $x_l \in [0.45, 0.55]$. That means that $\Delta x^{SPH} = 0.02m$ and $\Delta x^{FV} = 0.002m$. The discretization size of the FV cells is ten times smaller than the discretization size of the particles. This corresponds to the fact that we want to use the FV mesh to obtain a refined solution. In our future applications, the refined FV mesh often will be used to simulate the boundary layer. In this case the mesh size will be much

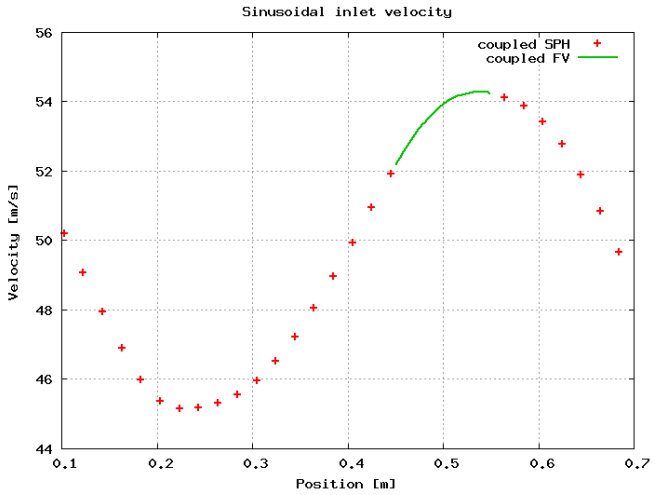

Figure 5: Velocity of a coupled one-dimensional simulation. A sinusoidal velocity is imposed at the inlet situated on the left hand side ($x = 0$), while constant static pressure is imposed at the outlet ($x = 1$). The green line indicates the solution obtained by the Finite Volume method, while the red points represent the SPH particles in Lagrangian motion.

smaller than the particle size. In Figure 5 it can be seen that the sinusoidal velocity is transferred without any problems from the SPH to FV domain and back again to the SPH particles.

4.2 Shock tube

The above testcase illustrates that the coupling correctly transfers information for Lagrangian moving particles. This case shows an example of how the coupling can be used to achieve a more accurate solution with an equal number of calculation points. We consider the one dimensional shock tube testcase presented in [12, 13]. The initial data was chosen according to [12] with a density discontinuity in the middle of the domain at $x = 0.5$,

$$\begin{cases} \rho_L = 1100, & v_L = 0, \\ \rho_R = 1000, & v_R = 0, \end{cases}$$

with the reference density $\rho_0 = 1000$ and the reference speed of sound $c_0 = 1450$. The analytical solution is known and consists of a rarefaction wave travelling from the discontinuity to the left and a shock wave travelling to the right. In addition, a coarse (1000 SPH particles) and a refined (5000 SPH particles) SPH reference solution have been computed. Using the same number of calculation points as for the coarse SPH solution, a coupled simulation is launched with 800 SPH particles in the whole computational domain and 200 FV cells equally distributed in $x_l \in [0.48, 0.52]$. The discretization size of the FV cells corresponds to the discretization size of the refined SPH simulation. Figure 6 and 7 show

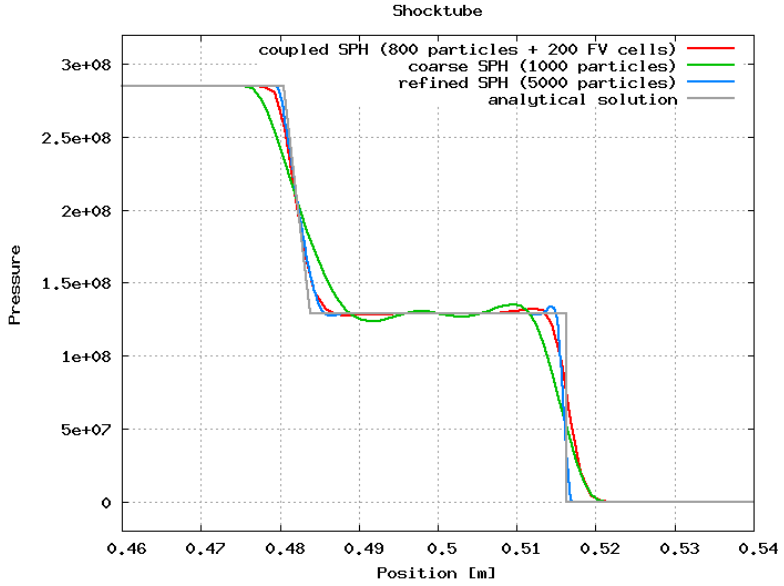

Figure 6: Pressure of the shock tube testcase computed by a coarse and a refined SPH simulation compared to a coupled SPH-FV solution with 800 SPH particles and 200 FV cells. The FV domain is situated in $x_l \in [0.48, 0.52]$.

that the coupled solution is much more accurate than the coarse SPH simulation that uses the same number of calculation points because the points for the coupled simulation are refined around the initial discontinuity. This illustrates how the coupling will be applied to real industrial applications in the future.

5 CONCLUSIONS

A novel coupling algorithm of an SPH-ALE and a FV method was presented. The fields computed in the more accurate FV domain are transferred to the SPH domain by using the FV calculation points as SPH neighbors. Interpolation from SPH particles determines the boundary conditions for the FV domain. The approach shows very encouraging results for acadamic one-dimensional testcases and no obstacle has been identified for its successful implementation in two or three space dimensions. For the industrial applications, that we are interested in, it will be indispensable to include the simulation of viscous phenomena into the approach.

ACKNOWLEDGMENT

The authors would like to thank the ANRT (Association Nationale Recherche Technologie), Thèse 1120/2010, the CIRT (Consortium Industrie-Recherche en Turbomachines) and the European Reintegration Grant ERG (No. 267072). Many thanks to the colleages of the R&D department of ANDRITZ Hydro Vevey (Switzerland) for their support.

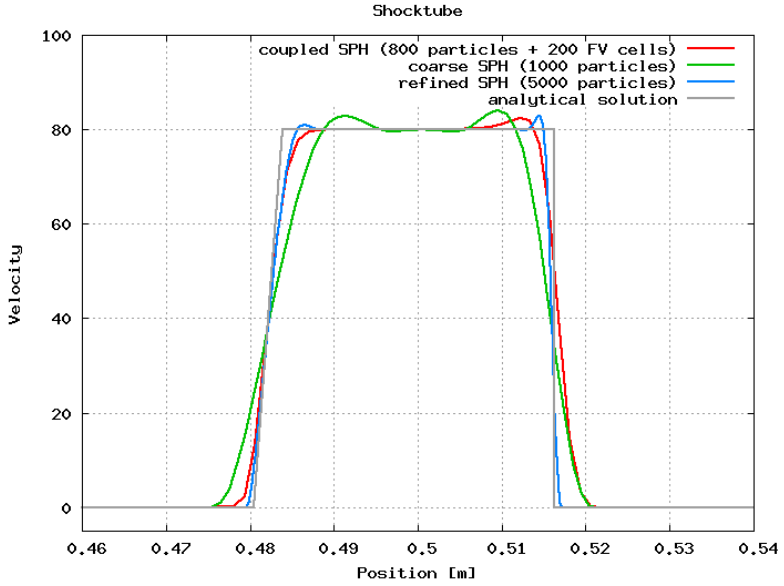

Figure 7: Velocity of the shock tube testcase computed by a coarse and a refined SPH simulation compared to a coupled SPH-FV solution with 800 SPH particles and 200 FV cells. The FV domain is situated in $x_l \in [0.48, 0.52]$.

We would like to express our gratitude to Prof. Francis Leboeuf who passed away much too early. We are deeply thankful to the scientist and to the wise man for the years of friendly collaboration.

REFERENCES

[1] M. Neuhauser, F. Leboeuf, J.-C. Marongiu, E. Parkinson, and D. Robb. Simulations of rotor-stator interactions with SPH-ALE. In *Advances in Hydroinformatics (In press)*, 2014.

[2] E. Parkinson, A. Karakolcu, N. Gervais, M. Rentschler, and K. Winkler. Recent development in the hydraulics of Pelton turbines. In *HYDROVISION India*, 2012.

[3] L.B. Lucy. A numerical approach to the testing of the fission hypothesis. *Astronomical Journal*, 82:1013–1024, 1977.

[4] R.A. Gingold and J.J. Monaghan. Smoothed particle hydrodynamics: Theory and application to non-spherical stars. *Mon. Not. R. astr. Soc.*, 181:375–389, 1977.

[5] J.P. Vila. On particle weighted methods and smooth particle hydrodynamics. *Mathematical Models and Methods in Applied Sciences*, 9:161–209, 1999.

[6] J. Leduc, F. Leboeuf, M. Lance, E. Parkinson, and J.-C. Marongiu. Improvement of multiphase model using preconditioned Riemann solvers. In *5th Int. SPHERIC Workshop, Manchester (England)*, 2010.

[7] J.-C. Marongiu, F. Leboeuf, and E. Parkinson. Riemann solvers and efficient boundary treatments: an hybrid SPH-finite volume numerical method. In *3rd Int. SPHERIC Workshop, Lausanne (Switzerland)*, 2008.

[8] C. Hirsch. *Numerical Computation of Internal and External Flows. Volume 1. Fundamentals of Numerical Discretization*. John Wiley and Sons Ltd., 1988.

[9] A. Amicarelli, J.C. Marongiu, F. Leboeuf, J. Leduc, M. Neuhauser, L. Fang, and J. Caro. SPH truncation error in estimating a 3D derivative. *International Journal for Numerical Methods in Engineering*, 87:677–700, 2011.

[10] J.A. Benek, J.L. Steger, and F.C. Dougherty. A flexible grid embedding technique with application to the Euler equations. *AIAA Papers*, 83-1944:373–382, 1983.

[11] E. Part-Enander and B. Sjogreen. Conservative and non-conservative interpolation between overlapping grids for finite volume solutions of hyperbolic problems. *Computer & Fluids*, 23:551–574, 1994.

[12] J. Leduc. *Etude physique et numérique de l'écoulement dans un système d'injection de turbine Pelton*. PhD thesis, LMFA, EC Lyon, 2010.

[13] J.-C. Marongiu. *Méthode numérique lagrangienne pour la simulation d'écoulements à surface libre - Application aux turbines Pelton*. PhD thesis, LMFA, EC Lyon, 2007.